Soil Dynamics and Earthquake Engineering 172 (2023) 107995

Contents lists available at ScienceDirect

Soil Dynamics and Earthquake Engineering

journal homepage: www.elsevier.com/locate/soildyn

Particle swarm optimization of friction tuned mass dampers subjected to ground motion records

Boshra Besharatian [a], Hossein Tajmir Riahi [a], Reyes Garcia [b,*], Iman Hajirasouliha [c]

[a] Department of Civil Engineering, University of Isfahan, Isfahan, Iran
[b] Civil Engineering Stream, School of Engineering, The University of Warwick, Coventry, UK
[c] Department of Civil and Structural Engineering, The University of Sheffield, Sheffield, UK

ARTICLE INFO

Keywords:
Friction tuned mass damper
Structural control
Single degree of freedom
Particle swarm optimization
Ground motion excitation
Multi-story frames

ABSTRACT

Friction tuned mass dampers (FTMDs) are widely used to control the displacement of structures located in seismically active areas. Typically, the frequency and friction ratios of FTMDs are tuned up during design, but this task is complex if real ground motion records are considered. This article proposes a novel and accurate approach to calculate optimum parameters of FTMDs for controlling the displacements of both single degree of freedom (SDOF) systems and multi-story structural frames subjected to real ground motion records. In this study, the SDOF displacement and two FTMD parameters (frequency ratio and friction ratio) are first optimized simultaneously using a Particle Swarm Optimization (PSO) algorithm. A series of sensitivity analyses are then carried out to examine the effect of different structural features (damper movement, variations of optimized parameters and damping) on the optimized SDOF displacements and FTMD parameters given by the PSO. It is shown that, compared to a more established method available in the literature, the PSO algorithm reduces the SDOF displacements by an additional 21% on average. The PSO is then used to obtain optimum parameters of FTMDs and TMDs connected to four moment-resisting frames, and the results from the frames are compared to those from equivalent SDOF systems. This article contributes towards providing more suitable optimization tools for structures fitted with FTMDs, which in turn can lead to more efficient design methods for dampers.

Author statement

Boshra Besharatian: Formal analysis, Investigation, Methodology, Software, Writing- Original draft preparation. **Hossein Tajmir Riahi**: Conceptualization, Supervision, Validation, Writing- Original draft preparation. **Reyes Garcia**: Conceptualization, Visualization, Writing- Reviewing and Editing. **Iman Hajirasouliha**: Writing- Reviewing and Editing.

1. Introduction

Tuned mass dampers (TMDs) are used in structures to reduce the vibrations induced by strong earthquakes. Traditionally, TMDs are fitted with viscous damping elements that help the damper remain in the linear (elastic) stage, thus simplifying its design. However, TMDs tend to be expensive, which in turn hinders their wide adoption in the structural control of structures. Moreover, traditional TMDs with viscous damping elements are prone to aging and their behavior is temperature-dependent. To bypass these drawbacks, friction tuned mass dampers (FTMDs) with dry friction elements were proposed in the past [1]. The use of a friction damping mechanism in the damper has practical advantages such as ease of implementation, low cost and minimal maintenance. In general, FTMDs can be grouped into two types: i) translational FTMDs, in which the damper moves parallel to the movement of the main structure and dissipates energy through an elasto-plastic force, and ii) pendulum FTMDs, in which the mass of the damper moves (rolls or slides) on a surface by taking advantage of gravity.

Previous research has examined the effectiveness of translational FTMDs at controlling the response of structures. For instance, Ricciardelli and Vickery [2] investigated the steady state response of a single degree of freedom (SDOF) structure with a TMD with linear stiffness and dry friction elements (which is essentially a FTMD). Ricciardelli and Vickery also proposed closed-form expressions to calculate the optimized FTMD parameters (based on minimum structural displacements as objective function) when the system was subjected to harmonic force.

* Corresponding author.
E-mail address: reyes.garcia@warwick.ac.uk (R. Garcia).

https://doi.org/10.1016/j.soildyn.2023.107995
Received 13 December 2022; Received in revised form 22 April 2023; Accepted 25 April 2023
Available online 16 May 2023

Nasr et al. [3] subsequently reformulated Ricciardelli and Vickery expressions for a system with viscous damping. Lee et al. [4] demonstrated that, with a proper design, FTMDs can have both mass damper and friction damper characteristics, thus enhancing its structural performance. Lin et al. [5,6] studied semi-active FTMD models and proved experimentally that their adopted solution was effective at controlling vibrations in SDOF structures. FTMDs also proved effective at mitigating the vibrations of bladelike structures, but only when these structures are lightly damped [7]. On the other hand, pendulum-type FTMDs have been less studied [8–12] mainly due to their complexity in design and construction. For example, Chung et al. [13] presented optimal design solutions for friction pendulum tuned mass damper with varying friction coefficients. Past studies have also examined the effect of the type of load on the response of structures fitted with FTMDs. Gewei and Basu [14] analyzed SDOF systems with FTMDs subjected to harmonic load. Pisal and Jangid [15] investigated the influence of the FTMDs' main parameters on the response of SDOFs subjected to harmonic excitations and ground motion records. Dogan and Cigeroglu [16] used the harmonic balance method to obtain steady state solutions of two TMDs equipped with dry friction dampers in the frequency domain. Kim and Lee [17] used four configurations of frictional multiple tuned mass dampers (FMTMDs) and discussed their practical applications. Whilst the understanding the performance of FTMDs subjected to ground motion excitations is necessary to determine the effectiveness of such devices, only a few studies have actually focused on this aspect [18–20]. Moreover, FTMDs tend to behave in a nonlinear manner when controlling vibrations. Such nonlinear behavior complicates the calculation of a system's response because the simple mathematical methods used to analyze TMDs cannot be applied to FTMDs.

In real practice, the main parameters of TMDs (i.e. mass, stiffness and damping) have to be optimized during design to meet an optimum level of response. Previous research has successfully optimized the parameters of TMDs using classical methods [21–24]. However, while such methods can be easily applied to periodic excitations (e.g. sinusoidal), their application to random excitations (e.g. ground motion records) is not trivial. Other alternative techniques have been proposed to optimize the TMDs parameters including: genetic algorithms [25], bat algorithms [26], ant colony algorithms [27], flower pollination algorithms [28], and harmony searches [29]. Bakre and Jangid [30] extracted optimum parameters for damped SDOF systems using harmony search algorithms and compared their results with classical closed-form mathematical solutions. Likewise, Marano et al. [31] proposed an approach to optimize the parameters of TMDs but the damper's mass was kept as a variable in the optimization process. Marano et al. concluded that the optimized damper's mass was too large and thus unachievable in real practice, which suggests that the damper's mass can be fixed (within reasonable values) during design. Particle Swarm Optimization (PSO) has also proved successful in TMD optimization problems [32,33]. Compared to other evolutionary algorithms [e.g. genetic algorithms (GA) or ant colony optimization (ACO)], PSO has prominent features such as simplicity in implementation, few parameters to set, and high convergence speed [34]. As a result, PSO is an attractive option to optimize the main parameters of FTMDs that requires further investigation.

This article proposes a novel and accurate approach based on PSO to calculate optimum parameters of FTMDs for controlling the displacements of both single degree of freedom (SDOF) systems and multi-story structural frames subjected to real ground motion records. First, a parametric study is performed to examine the effect of mass ratio, frequency ratio and friction ratio on the displacement of SDOFs fitted with FTMDs. Subsequently, a PSO algorithm is used to optimize the SDOF displacement and the main parameters of the FTMDs. For comparison, the parameters of TMDs are also optimized. The results are discussed in terms of the dampers' optimum response, optimum damper parameters, and sensitivity of the response to changes in the properties of the SDOFs and FTMDs. The results from the optimization are also compared with those from an existing optimization approach available in the literature. Finally, the same PSO procedure is used to obtain optimum parameters of FTMDs and TMDs connected to four multi-story moment-resisting frames. These optimum parameters are compared with their corresponding values in equivalent SDOF systems. This article contributes towards providing more suitable optimization tools for structures fitted with FTMDs, which in turn can lead to more efficient design methods for buildings fitted with dampers.

2. Structural model

Fig. 1 shows schematically the system analyzed in this study. The equations of motion of such system (assuming dynamic acceleration at the base) can be expressed by Eqs. (1a) and (1b).

$$m_s\ddot{x}_s + c_s\dot{x}_s + k_s x_s + k_d(x_s - x_d) = -m_s\ddot{x}_g(t) + f_s sgn(\dot{x}_d - \dot{x}_s) \tag{1a}$$

$$m_d\ddot{x}_d - k_d(x_s - x_d) = -m_d\ddot{x}_g(t) - f_s sgn(\dot{x}_d - \dot{x}_s) \tag{1b}$$

where m_s, k_s and c_s are the corresponding mass, stiffness and damping ratio of the SDOF structure, respectively; m_d and k_d are the mass and stiffness of the FTMD, respectively; f_S is the friction force mobilized between the damper and the SDOF structure; *sgn* represents the sign function; and $\ddot{x}_s$, $\dot{x}_s$ and x_s are the acceleration, velocity and displacement of the main structure. Likewise, $\ddot{x}_d$, $\dot{x}_d$, x_d represent the acceleration, velocity and displacement of the damper, respectively. Note that the term $(x_s - x_d)$ in the above equations represents the relative displacement of the damper with respect to the main structure.

Eqs. (1a) and (1b) can be rewritten in matrix form as:

$$\boldsymbol{M}\ddot{\boldsymbol{X}}(t) + \boldsymbol{C}\dot{\boldsymbol{X}}(t) + \boldsymbol{K}\boldsymbol{X}(t) = \boldsymbol{E}\ddot{x}_g(t) + \boldsymbol{B}F_S(t) \tag{2}$$

$$\boldsymbol{X}(t) = \begin{Bmatrix} x_s(t) \\ x_d(t) \end{Bmatrix} \tag{3}$$

where $\boldsymbol{M}$, $\boldsymbol{K}$ and $\boldsymbol{C}$ are the mass, stiffness and damping matrices of the system, respectively; $\boldsymbol{E}$ and $\boldsymbol{B}$ are the placement vectors for excitation and friction forces; $\boldsymbol{X}(t)$, $\dot{\boldsymbol{X}}(t)$ and $\ddot{\boldsymbol{X}}(t)$ are the displacement, velocity and acceleration of the system, respectively; $\ddot{x}_g(t)$ is the ground acceleration; $F_S(t)$ is the friction force produced by the FTMD; and $x_s(t)$ and $x_d(t)$ are the relative displacements between the ground and the SDOF structure and the FTMD, respectively (see Fig. 1). $\boldsymbol{M}$, $\boldsymbol{K}$, $\boldsymbol{C}$, $\boldsymbol{E}$, and $\boldsymbol{B}$ can be calculated using Eqs. (4)–(8), whereas $F_S(t)$ can be computed using Eq. (9):

$$\boldsymbol{M} = \begin{bmatrix} m_s & 0 \\ 0 & m_d \end{bmatrix} \tag{4}$$

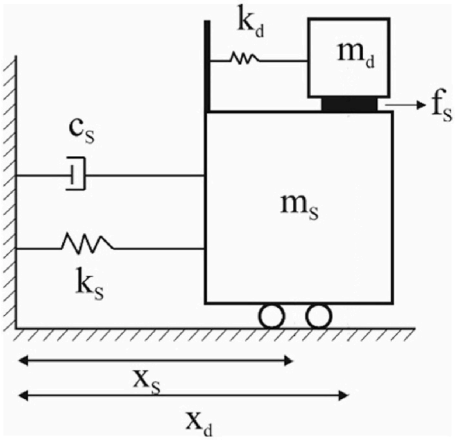

Fig. 1. FTMD and SDOF system used in this study.

$$\boldsymbol{C} = \begin{bmatrix} c_s & 0 \\ 0 & 0 \end{bmatrix} \tag{5}$$

$$\boldsymbol{K} = \begin{bmatrix} k_s + k_d - k_d \\ -k_d \quad k_d \end{bmatrix} \tag{6}$$

$$\boldsymbol{E} = \begin{bmatrix} -m_s \\ -m_d \end{bmatrix} \tag{7}$$

$$\boldsymbol{B} = \begin{bmatrix} 1 \\ -1 \end{bmatrix} \tag{8}$$

$$F_s(t) = f_s sgn(\dot{x}_d(t) - \dot{x}_s(t)) \tag{9}$$

In this study, the FTMD parameters are defined through a mass ratio μ, a frequency ratio f, and a friction ratio R_f, as shown in Eqs. (10)–(12) [14,15]:

$$\mu = m_d / m_s \tag{10}$$

$$f = \omega_d / \omega_s \tag{11}$$

$$R_f = \frac{f_s}{m_d \times g} \tag{12}$$

where $\omega_d = \sqrt{k_d/m_d}$ and $\omega_s = \sqrt{k_s/m_s}$ are the frequencies of the damper and the SDOF structure, respectively; g is the acceleration of gravity. The rest of the variables are as defined before.

3. Parametric analysis

Based on the system shown in Fig. 1, a parametric analysis was carried out to examine how the FTMD parameters change the displacement of SDOF structures. The SDOF structures had structural periods T_s = 0.5, 1.0 or 2.0 s (where $T_s = 2\pi/\omega_s$), which are representative of regular low-, mid- and high-rise buildings. It is assumed here that such buildings are controlled predominantly by their 1st mode of vibration. The building mass was assumed to be 10,000 kg. Each system was examined using three mass ratios μ = 0.01, 0.03 or 0.05, which represent practical values used in real projects and in previous studies [9,15]. It should be noted that the mass of FTMDs depends on practical and economic considerations, and as such the mass ratio is limited to values within those proposed above. In practical applications, the mass ratio of TMD in high-rise buildings rarely exceeds 0.5% of the total mass of the structure [35]. Therefore, in order to improve the performance of TMDs, the tuned mass damper inerter has been developed as a lower-mass alternative to conventional TMDs [36,37]. Clearly, these innovations should also be considered for FTMD to result in a significant reduction of the attached mass.

The systems were modeled and analyzed in OpenSees software [38]. An elastic material was used to model the stiffness (k_d) of the FTMDs, whereas a rigid-plastic material was used to model the friction between the FTMDs and the SDOF structures (see Fig. 2). A set of 20 real ground motion records from the SAC project were selected for the analyses [39]. All records had a probability of exceedance of 10% in 50 years for Los Angeles, as summarized in Table A.1 of Appendix A. The mean spectral acceleration of the set of records matches well the ASCE-07 design spectrum, which is consistent with current design practice. During the analyses, the ground motion records were applied to the base of the SDOF structures.

Fig. 3 shows the (mean) maximum displacement of the SDOF structures ($x_{s,ave}$) as a function of the frequency ratio f and friction ratio R_f for the three mass ratios μ = 0.01, 0.03 and 0.05 adopted in this study. The plots in Fig. 3 present values of R_f ranging from 0.015 to 0.5, and values f ranging from 0.015 to 0.5, both with increments of 0.015. The results in Fig. 3 were obtained using a constant value ω_s and a variable value ω_d, as well as a damping ratio ξ_s = 0.02 ($\xi_s = c_s\omega_s/2k_s$) which is representative of structures fitted with dampers. The results in Fig. 3 confirm previous research that showed that $x_{s,ave}$ reduces if the frequency of the FTMDs is close to the frequency of the SDOF structure. Indeed, the smallest values of displacements $x_{s,ave}$ occur at ranges of f = 0.8–1.1, but more evidently at $f \approx 1$. Note also that the maximum displacements $x_{s,ave}$ of uncontrolled (i.e. without FTMDs) SDOF structures with T_s of 0.5, 1.0 and 2.0 s are around 95, 300 and 415 mm, respectively.

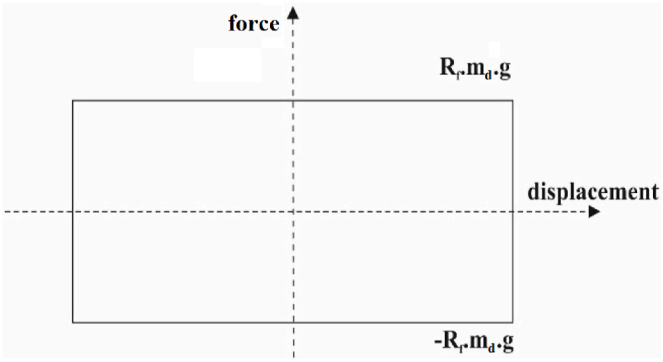

Fig. 2. Force-displacement model in friction phase of FTMDs.

The results in Fig. 3 show that, for the three structural periods T_s considered in the analyses, the displacements $x_{s,ave}$ reduce as the mass ratio μ increases. However, the reduction in $x_{s,ave}$ is less significant as μ increases. Fig. 3 also shows that R_f varies from 0 to 0.5, thus suggesting that the friction ratio (as a variable parameter of FTMDs) is affected by both the structure and damper parameters. However, for the studied systems, the optimum value of R_f is always less than 0.2. The results in Fig. 3 also indicate that, in some cases, the controlled and uncontrolled responses of the analyzed system are similar. For instance, a system with T_s = 1.0 s, μ = 0.01, f = 1.5 and R_f = 0.5 experiences a displacement $x_{s,ave}$ = 229 mm, which is the same displacement that the main system would experience in an uncontrolled state. This proves the importance of selecting the optimized FTMD parameters, as the damper may not change the response of the system if the parameters are not optimized.

The results from the parametric analysis confirm that the FTMDs' parameters (mainly the frequency ratio f and friction ratio R_f) influence heavily the displacements of the SDOF structure. Moreover, such parameters also depend on the SDOF structure's properties, which in turn complicates the design of FTMDs. Accordingly, the following section implements a Particle Swarm Optimization (PSO) algorithm aimed to find optimum damper parameters that lead to the smallest SDOF displacements $x_{s,ave}$. It should be mentioned that, whilst the interpretation of results in Fig. 3 seems straightforward, the results are clearly different for the different systems. For example, FTMDs with μ = 0.03 have different performances to the rest of systems. It is also evident that there is not monotonicity in their boundaries for two parameters. Moreover, Fig. 3 only presents the case studies examined in this article and clearly the results may be different for other structural periods. Consequently, it is not possible to use boundary search techniques because a robust method to deal with different types of performances is required in the analysis. Whilst boundary search techniques with more general approaches could be adopted in the analysis, it is considered that such techniques do not give a significant advantage over PSO methods and therefore the latter are adopted in this study.

4. Particle swarm optimization (PSO) process

In essence, a PSO algorithm is characterized by the position and velocity of a particle in a d-dimensional space. Thus, every particle in the swarm is defined by a position vector $X_i = [x_{1,i}, x_{2,i}, \ldots, x_{d,i}]$, and by a

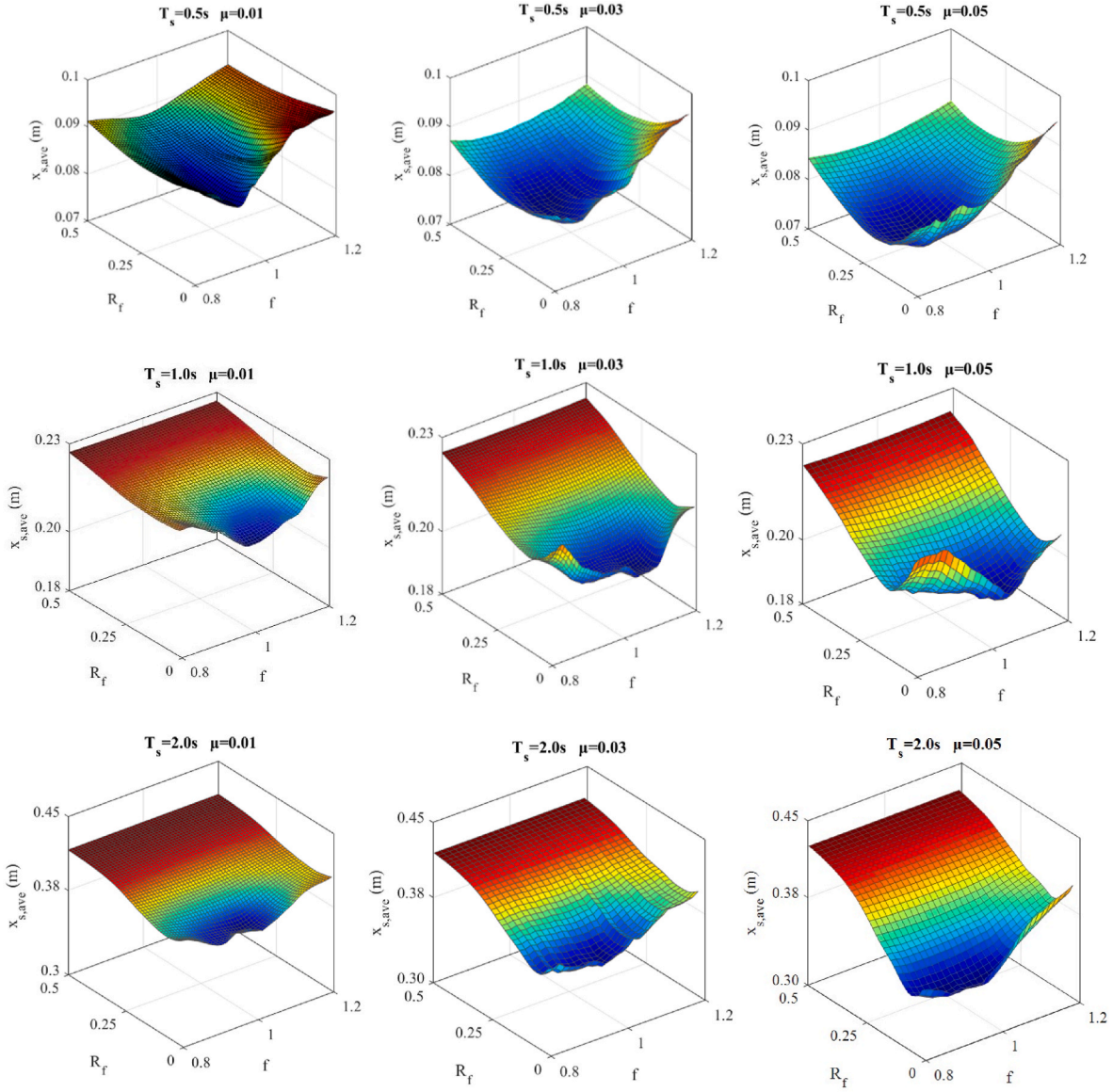

Fig. 3. Mean maximum displacement ($x_{s,\text{ave}}$) of SDOFs as a function frequency ratio f and friction ratio R_f for mass ratios a) $\mu = 0.01$, b) $\mu = 0.03$, and c) $\mu = 0.05$.

velocity vector $V_i = [v_{1,i}, v_{2,i}, \ldots, v_{d,i}]$. Particles also keep their own best position experience $P_i = [p_{1,i}, p_{2,i}, \ldots, p_{d,i}]$ during the process, according to the objective function of optimization. A global best position P_g is also defined, which is a shared component between all the particles in the swarm.

The PSO algorithm was implemented in Matlab® in order to link it to the systems modeled in OpenSees (shown in Fig. 1). To compare the effectiveness of FTMDs to other solutions, equivalent TMDs were also optimized. TMDs are used as a benchmark mainly because their behavior is similar to that of FTMDs, and also because TMDs are a more established solution for structural control. The aim of the optimization was to obtain the optimized parameters of both FTMDs (i.e. frequency ratio f and friction ratio R_f) and TMDs (i.e. frequency ratio f and viscous damping ratio ξ_T) that led to the minimum mean displacement $x_{s,\text{ave}}$ of the SDOF structure. The optimization was repeated for five mass ratios $\mu = 0.01$, 0.03, 0.05, 0.07 and 0.10, and for eight periods $T_s = 0.3$, 0.5, 0.7, 1.0, 1.5, 2.0, 3.0 and 4.0 s. Accordingly, 80 different systems were optimized using the set of 20 ground motion records.

The implementation of the PSO algorithm on the investigated systems follows the general steps below, also summarized in Figure A1 of Appendix A:

Step 1) Determine the objective function: This was done to find the damper parameters that minimized the maximum average displacement $x_{s,\text{ave}}$ of the SDOF structure when subjected to the full set of ground motion records. The value $x_{s,\text{ave}}$ is used here because drifts are extensively used in structural control. It should be noted that other parameters such as the acceleration response of the structures, their energy dissipation capacity or any combination between these parameters can be used as objective function that may result in a better performance [40–42]. The minimization of the maximum average displacement was used here as an example to investigate the effectiveness of the PSO algorithm.

Step 2) Determine the target space: The optimization variables were f and R_f for systems fitted with FTMDs, or f and ξ_T for systems with TMDs. This led to two-dimensional spaces. Based on the results from Section 3, the values of f and R_f are set to $0.65 \leq f \leq 1.15$ and $0.0 \leq R_f \leq 0.4$ for the periods T_s considered in the analyses. Note that the value of the mass ratio μ is not optimized because its value is limited by practical constraints (e.g. space restrictions for FTMD's installation, complexity in construction, material costs etc.). Therefore, the mass ratio is set to a maximum value of $\mu = 0.1$ in the optimization process.

Step 3) Specify characteristics of the adopted algorithm: The population of particles and the number of iterations are selected to be 5 and 25, respectively. The final values of these two parameters were selected by trial and error until a change (increase) in their magnitudes no longer influenced the optimized results.
Step 4) Initialization: Random position values are assigned to each particle based on the target space.
Step 5) Evaluate objective values: Based on the objective values of each particle, the best experienced position of the particles is extracted, as well as the best position experienced by the entire swarm.
Step 6) Update velocity and position of particles: The velocity and position of the particles are updated by using Eqs. (13) and (14), respectively.

$$v_{ij}[t+1] = w\, v_{ij}[t] + c_1\, r_1\, \left(p_{ij} - x_{ij}[t]\right) + c_2 r_1\, \left(g_j - x_{ij}[t]\right) \quad \mathrm{j} = 1,2 \tag{13}$$

$$x_{ij}[t+1] = x_{ij}[t] \times v_{ij}[t+1] \tag{14}$$

where $v_{ij}[t+1]$ and $x_{ij}[t+1]$ are the velocity and position to be applied to the ith particle in the next step; $v_{ij}[t]$ is the current velocity of the particle; $x_{ij}[t]$ is the current position of the particle; r_1 and r_2 are random vectors with the same size of problem variables (with values between 0 and 1) that help the convergence; w, c_1 and c_2 are the acceleration of the particle's motion in its current direction, the acceleration of the particle's motion towards its best position, and the acceleration of the particle's motion towards the best global position of the particles, respectively. The current study adopted the optimized values for a multidimensional space proposed by Clerc and Kennedy [43]: $w = 2.05$, $c_1 = 0.73$ and $c_2 = 0.73$.

Step 7) Update the particles' best position and global best position: The responses taken from the new position and velocity of particles are compared with the current particles' best position and global best position to find the best position.
Step 8) Iteration: Steps 5 to 7 are repeated based on a certain number of iterations. The number of iterations was adjusted by trial and error and set equal to 140.
Step 9) Extract the global best position and its objective values: These parameters correspond to the optimum value of the objective function and the optimized damper parameters f and R_f (or f and ξ_T).

The following section presents and discusses the results of the adopted optimization process.

5. Results and discussion

5.1. Maximum displacements of optimized systems with FTMDs and TMDs

Table 1 compares the maximum mean displacements $x_{s,\mathrm{ave}}$ of the SDOF structures fitted with FTMDs or TMDs, as well as the reduction in

Table 1
Mean displacements of systems without (uncontrolled) or with TMDs and FTMDs.

T_s (s)	μ	Uncontrolled system	FTMD			TMD		
		$x_{s,\mathrm{ave}}$ (mm)	$x_{s,\mathrm{ave}}$ (mm)	Reduction (%)	Average Reduction (%)	$x_{s,\mathrm{ave}}$ (mm)	Reduction (%)	Average Reduction (%)
0.25	0.01	27.7	24.0	13.2	16.7	23.5	15.2	22.7
	0.03		23.2	16.0		21.9	20.8	
	0.05		22.6	18.3		21.0	24.1	
	0.07		23.0	17.0		20.5	25.8	
	0.10		22.4	18.9		20.0	27.7	
0.5	0.01	95.1	81.8	14.0	22.5	80.9	14.9	25.5
	0.03		75.8	20.3		72.9	23.4	
	0.05		72.8	23.5		69.6	26.8	
	0.07		70.4	26.0		66.9	29.6	
	0.10		67.9	28.6		63.9	32.8	
0.75	0.01	156.4	141.6	9.4	15.3	140.7	10.0	17.8
	0.03		134.6	13.9		131.4	16.0	
	0.05		131.4	16.0		126.4	19.2	
	0.07		128.9	17.6		124.0	20.7	
	0.10		125.9	19.5		120.6	22.9	
1.0	0.01	228.6	209.3	8.4	15.1	208.0	9.0	18.2
	0.03		195.5	14.5		191.2	16.4	
	0.05		189.6	17.1		182.0	20.4	
	0.07		189.0	17.3		178.8	21.8	
	0.10		186.9	18.2		175.5	23.2	
1.5	0.01	344.0	301.9	12.2	20.1	298.9	13.1	22.3
	0.03		284.1	17.4		277.9	19.2	
	0.05		270.1	21.5		263.1	23.5	
	0.07		263.2	23.5		253.5	26.3	
	0.10		254.8	25.9		242.9	29.4	
2.0	0.01	415.8	377.4	9.3	17.1	375.3	9.7	18.5
	0.03		349.4	16.0		346.3	16.7	
	0.05		338.8	18.5		333.8	19.7	
	0.07		332.9	19.9		324.1	22.1	
	0.10		325.5	21.7		314.7	24.3	
3.0	0.01	638.6	581.2	9.0	18.1	579.9	9.2	19.7
	0.03		538.8	15.6		534.6	16.3	
	0.05		512.5	19.7		501.7	21.4	
	0.07		499.2	21.8		483.2	24.3	
	0.10		482.2	24.5		464.6	27.2	
4.0	0.01	649.5	612.9	5.6	12.6	613.0	5.6	13.7
	0.03		580.0	10.7		577.0	11.1	
	0.05		560.3	13.7		551.0	15.2	
	0.07		547.9	15.6		536.0	17.5	
	0.10		538.4	17.1		524.0	19.2	

displacements with reference to equivalent uncontrolled structures. The results show that, as expected, both FTMDs and TMDs reduce $x_{s,ave}$ when compared to uncontrolled counterpart systems. Compared to the FTMDs, the TMDs are slightly more effective at reducing $x_{s,ave}$ for all mass ratios μ. However, the reduction depends on the period T_s. For example, if all mass ratios are considered, the displacements $x_{s,ave}$ of systems with TMDs and $T_s = 0.25$ s are only 6% smaller than that those of the equivalent systems with FTMDs. Note also that structures with $T_s = 0.5$ s experience the largest reductions in $x_{s,ave}$, but such reductions are small for long-period structures with $T_s = 4.0$s. Moreover, as the period T_s elongates, the reductions in $x_{s,ave}$ are very similar regardless of whether FTMDs and TMDs are fitted. This indicates that, for long-period structures, the damper mass influences more the reduction in $x_{s,ave}$ than the friction phase of the FTMD, or the viscous damping of the TMD.

Figs. 4a–b compare the optimum frequency ratios f of systems with FTMDs and TMDs for different values of T_s and μ. The results show that i) f tends to decrease as the mass ratio μ increases, and ii) f tends to vary in a similar way for both FTMDs and TMDs, which is consistent with the findings presented by Leung and Zhang [32]. For example, f tends to increase between $T_s = 2.0$ s and $T_s = 4.0$ s. Note also that the range of values of f is similar for both FTMDs and TMDs. For instance, for a system with $T_s = 0.5$ s and $\mu = 0.05$, both optimized FTMDs and TMDs resulted in a frequency ratio $f = 0.93$. This indicates that, although the energy dissipation mechanisms of these two types of dampers are different, their behavior is rather similar which in turn allows for comparisons between them (e.g. to perform sensitivity analyses to optimize values). The results in Fig. 4b also show that, for structures with T_s >1.5 s and fitted with TMDs, the optimum frequency ratio f decreases as the mass ratio μ increases. Overall, the range of optimum frequency ratios was found to be 0.78–1.07 for systems with FTMDs, and 0.81–1.06 for systems with TMDs. Based on these results, it is reasonable to adopt frequency ratios f between 0.9 and 1.0 for both FTMDs and TMDs in the analyses of idealized SDOF structures. It should be mentioned the scattered and oscillating trends of the frequency ratios in Figs. 4a-b can be attributed to the fact that the optimization is using a set of earthquake records. Indeed, a small change in a parameter can result in a large change in some records results, which leads to sudden changes in the optimum parameter because such a change can minimize the average response more effectively. This is different to cases when optimization is done for harmonic excitations or for single earthquake records, where the trends of the frequency rations (and other optimum parameters) are expected to be much smoother.

Fig. 5a compares optimum friction ratios R_f of the systems fitted with FTMDs for different values of T_s and μ. Likewise, Fig. 5b compares optimum viscous damping ratios ξ_T of counterpart systems with TMDs. Fig. 5a shows that as T_s elongates from 0.25 to 4.0 s, the mean value of R_f (over all mass ratios) decreases from 0.23 to 0.012. Also, for the different values T_s, the mean R_f increases (from 0.045 to 0.12) with the value of μ. These observations are also valid for Fig. 5b, where the optimum values of ξ_T in systems with TMDs follow a similar trend. The results in Figs. 5a–b highlight one of the main advantages of systems with FTMDs over systems with TMDs: for the mass ratios considered in the optimization, the scatter of R_f in FTMDs tends to be much smaller than the scatter of ξ_T in TMDs. The smaller scatter of R_f in systems with FTMDs can be advantageous in practical design situations, where the main damper parameters may need to be tuned up to match the project needs. However, note that for a constant mass ratio, the difference between optimum values of R_f is larger than the difference between optimum values of ξ_T.

5.2. Effect of damper movement and phase lag

The main energy dissipation mechanism in FTMDs and TMDs is the movement of the damper with a phase lag with respect to the movement of the structure. The study of the dampers' displacement is thus important towards designing these control devices in order to satisfy space limitations in structures. Table 2 compares the average displacements of the SDOF structure ($x_{d,ave}$) and the displacements of both optimized FTMDs and TMDs when the systems are subjected to the set of 20 seismic records. In this table, d_{FTMD} and d_{TMD} are the ratios of the mean displacements of the FTMDs and TMDs, respectively, over the mean displacement of the SDOF structure. Note that the results are shown for $T_s = 0.5$, 1.0 and 4.0 s as these are representative of regular low to high-rise buildings. The results show that, for both FTMDs and TMDs, the displacements of both the SDOF structure and dampers decrease as the mass ratio μ increases. However, as μ increases, the dampers' displacements reduce faster than the displacements of the SDOF structure, as indicated by decreasing values of d_{FTMD} and d_{TMD}. This implies that an increase in μ is more effective at reducing the dampers' displacement rather than the SDOF structure displacement. An additional consideration in the design is the stroke limits of TMDs and FTMDs. Long strokes need more room for installation. Fig. 1 shows that there is no limitation in the movement of m_d. Moreover, the variability of the friction coefficient between the static and dynamic phases was not considered in the numerical analysis. However, the strokes of TMDs and FTMDs strokes ($x_{d,ave} - x_{s,ave}$) were found to be within an acceptable range. Table 2 shows that for the worst-case scenario ($T_s = 4.0$ s and $\mu = 0.01$) the stroke would be about 4.5 m. This is deemed as achievable in tall buildings with large roof plans and TMDs and FTMDs fitted on them. Moreover, a limitation on the stroke can be added as a constraint in the PSO process.

Previous research [44] has shown that the phase deviation between

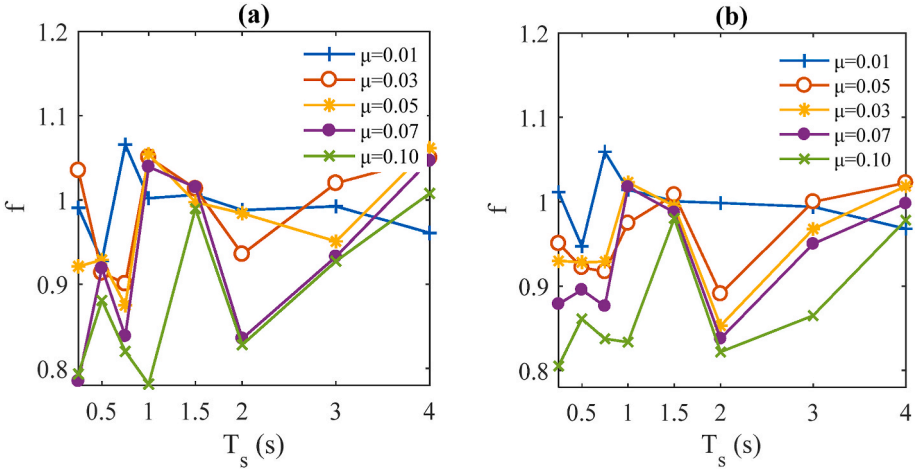

Fig. 4. Optimum frequency ratios f for systems with a) FTMDs, and b) TMDs.

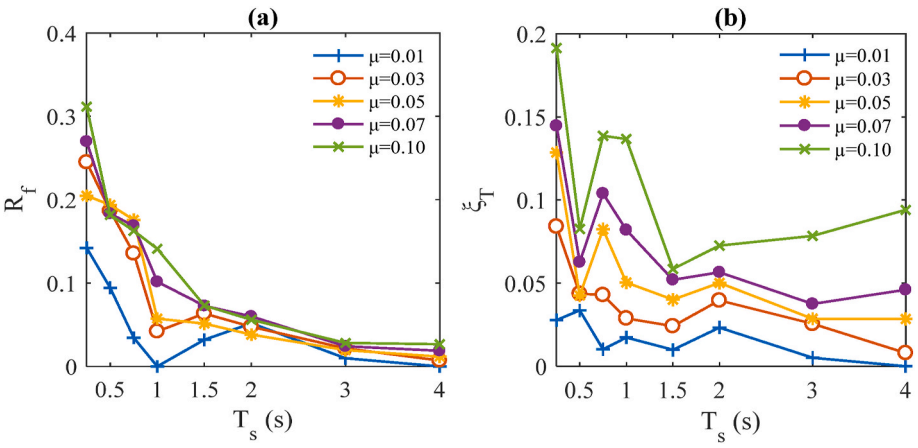

Fig. 5. Optimum values of a) friction ratio R_f for systems with FTMDs, and b) viscous damping ratio ξ_T for systems with TMDs.

Table 2
Comparison of displacements of dampers and SDOF structures.

T_s	μ	FTMD			TMD		
		$x_{d,ave}$ (mm)	$x_{s,ave}$ (mm)	d_{FTMD}	$x_{d,ave}$ (mm)	$x_{s,ave}$ (mm)	d_{TMD}
0.5	0.01	736.0	81.8	9.0	491.2	81.0	6.1
	0.03	568.8	75.8	7.5	333.7	73.3	4.6
	0.05	494.9	72.8	6.8	296.1	70.0	4.2
	0.07	436.3	70.4	6.2	248.0	67.1	3.7
	0.10	434.4	67.9	6.4	210.0	64.5	3.3
1.0	0.01	1507.1	209.3	7.2	1346.0	208.3	6.5
	0.03	1173.2	195.5	6.0	919.7	191.0	4.8
	0.05	929.1	189.6	4.9	688.3	182.6	3.8
	0.07	812.6	189.0	4.3	559.0	179.1	3.1
	0.10	729.0	186.9	3.9	458.8	175.6	2.6
4.0	0.01	5209.9	612.9	8.5	4906.4	613.3	8.0
	0.03	3248.0	580.0	5.6	2894.0	577.0	5.0
	0.05	2857.8	560.3	5.1	2060.1	551.4	3.7
	0.07	2520.2	547.9	4.6	1703.5	536.1	3.2
	0.10	2207.5	538.4	4.1	1287.0	524.0	2.5

the movements of the TMD and the main structure is critical at reducing vibrations. Indeed, a TMD is most effective at reducing vibrations when a 90° phase lag exists between the TMD's movement and the structure's movement. Due to the similar behavior of TMDs and FTMDs, it is expected that the latter will also be most effective at reducing vibrations at a 90° phase lag.

To investigate the phase lag of the investigated systems, Fig. 6a and c compare, respectively, the displacement histories of the optimized FTMDs and TMDs with the displacement of the SDOF structure with T_s = 0.5 s. Whilst Fig. 6 was obtained by subjecting the system to the Imperial Valley ground motion record (record LA01, PGA = 0.46 g), the following observations can be extended to the rest of the records. A close analysis of the displacement histories between 10 and 15 s (Fig. 6b) indicates that the phase lag at many displacement peaks is close to 90°. Moreover, the FTMD only moves if the SDOF displacements are significant (e.g. between 2 and 35 s in Fig. 6a and c). After 35 s, the FTMD and the SDOF structure move together since the input force from the earthquake cannot overcome the friction force of the FTMD. On the other hand, the TMD (Fig. 6d) essentially moves during the whole duration of the record. Note that the TMD keeps its secondary mass behavior and phase lag, and it also moves even at small SDOF displacements. This suggests that, since the TMD displaces more than the FTMD, the former damper would require more regular inspection and maintenance, which in turn would lead to higher operational costs for TMDs.

5.3. *Effect of variations in optimized parameters*

In real designs, the actual damper parameters can differ from the theoretical optimized values. This difference in the parameters has a

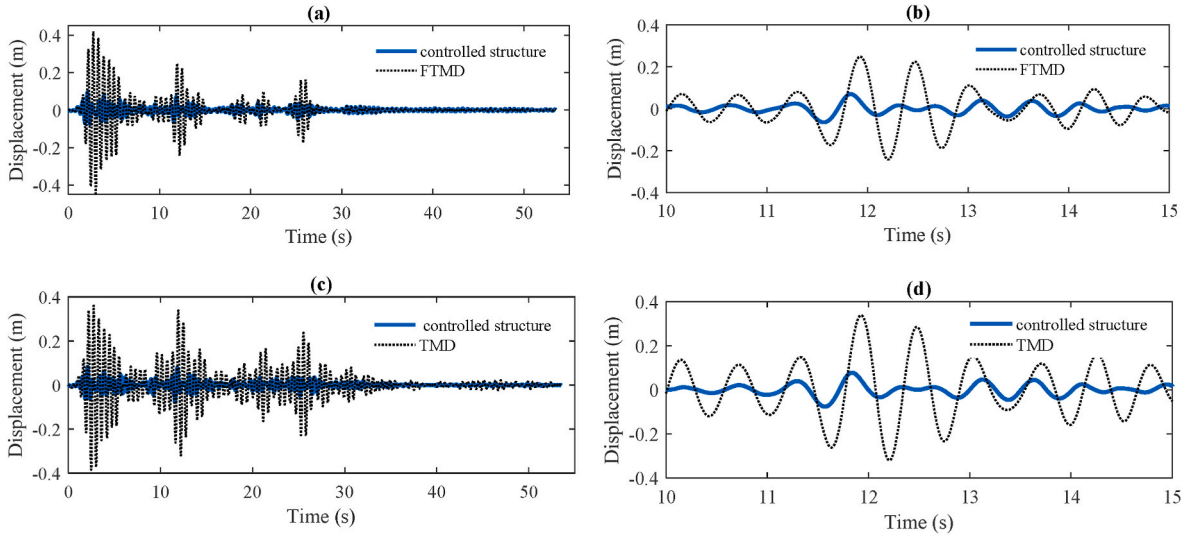

Fig. 6. Displacement of SDOF structure and (a)–(b) FTMD dampers, and (c)–(d) TMD dampers under Imperial Valley earthquake.

direct influence on the effectiveness of the damper at controlling vibrations. To assess the sensitivity of FTMDs and TMDs to variations in their optimized parameters (summarized in Table 3), three systems with $T_s = 0.5$, 1.0 and 4.0 s and $\mu = 0.05$ were analyzed. The responses of the SDOF structures were analyzed using a range of damper parameters, including the optimized values in Table 3 and their deviations from such values (from ±25% to ±50%). The sensitivity analysis was done using all the set of ground motions (20 records), and the results are the average of the responses.

Figs. 7a–c show the sensitivity of $x_{s,ave}$ to variations in the optimum frequency ratio f for the three systems. To get these results, the friction ratio R_f of FTMDs and damping ratio ξ_T of TMDs were set to their optimized values listed in Table 3. The results show that, in the case of FTMDs, the displacement $x_{s,ave}$ is less sensitive to variations of f. This is one of the main advantages of FTMDs over TMDs. For instance, in the case of $T_s = 0.5$ s (Fig. 7a), the maximum variation of $x_{s,ave}$ from the optimum value is 14% for a system with FTMDs, whereas such variation was 21% for the counterpart system with TMDs. However, as T_s elongated, $x_{s,ave}$ was similar for both systems with FTMDs and TMDs (Fig. 7c). Note also that some non-optimized values of f in FTMDs led to lower $x_{s,ave}$ when compared to equivalent non-optimized values of f in TMDs. It can be also noted that the optimized TMDs could reduce the mean displacement of the SDOF structure more than FTMDs, on average, by 6%.

Figs. 8a–c and Figs. 9a–c show, respectively, the sensitivity of $x_{s,ave}$ to variations in the optimized friction ratio R_f and viscous damping ratio ξ_T of the dampers. In these analyses, the parameters R_f and ξ_T were deviated ±50% from their optimized values, but the optimized value of f was kept as constant. The results in Fig. 8a–c and Fig. 9a–c indicate that, for values R_f and ξ_T higher than their optimum values, the displacement $x_{s,ave}$ varies with a smooth gradient. For example, for a structure with FTMDs and $T_s = 0.5$ s (Fig. 8a), the maximum variations of $x_{s,ave}$ corresponding to deviations of +50% and −50% from the optimized R_f are 2% and 4.3%, respectively. For an equivalent system with TMDs, such variations of $x_{s,ave}$ reduce to 0.25% and 1.4%, respectively. Based on the assumptions of this study, it is recommended that the friction ratio R_f and viscous damping ratio ξ_T are always chosen to be equal or higher than their optimized values. It should be added that, due to the inherent uncertainties of these parameters during the seismic response, it is not possible to suggest this for design purposes unless a comprehensive analysis is done for these parameters. Fig. 8a–c and Fig. 9a–c also show that, for the three systems examined, the optimum point given by the PSO process (marked with a black dot) coincides with the smallest $x_{s,ave}$ given by the sensitivity analysis, which confirms the effectiveness of the optimization procedure.

5.4. Effect of variations in the structure's damping ratio

In the analyses carried out in previous sections, the damping ratio of the SDOF structure was set to a ratio $\xi_S = 0.02$ as this value is often used in the design of structures with dampers. However, different structures can have different damping ratios. Figs. 10a–c shows the sensitivity of the optimized $x_{s,ave}$, f and R_f of systems with FTMDs to different damping ratios (ξ_S = 0.0, 0.01.0.02, 0.05 or 0.10) for different mass ratios μ. Figs. 11a–c also show comparable results ($x_{s,ave}$, f and ξ_T) but for systems with optimized TMDs. The results in Figs. 10a and 11a indicate that the optimum $x_{s,ave}$ follows consistent trends with variations in ξ_S and μ. For values ξ_S <0.05, small increments in the mass ratio μ leads to significant reductions in the displacement $x_{s,ave}$. However, for damping ratios $\xi_S \geq 0.05$, an increase in μ reduces $x_{s,ave}$ only marginally.

Figs. 10b and 11b show that the trend of the optimum frequency ratio f is similar for systems with FTMDs and TMDs. Overall, an increase in ξ_S leads to a reduction in f. Additionally, the results in Fig. 10c indicate that, in systems with FTMDs, the friction ratio R_f reduces as ξ_S increases. Note that the value of R_f tends to be approximately constant for mass ratios $\mu \geq 0.02$. Fig. 11c shows that the damping ξ_T of TMDs also reduces as ξ_S increases. However, ξ_T tends to increase as μ increases. A significant oscillation in ξ_T is evident for values of mass ratio $\mu \leq 0.05$. Such oscillation of results (also observed in Figs. 10b–c and Fig. 11b) can be attributed to the variable nature of the ground motion records used in the analyses.

The results in this section suggest that fitting FTMDs (and TMDs) on structures with low damping ratios ($\xi_S < 0.02$) is effective at reducing the structure's displacements. In this case, an increase in mass ratio leads to smaller structural displacements. Moreover, maximizing the value of the mass ratio in such structures is an attractive option to reduce the frequency ratio of the damper. Conversely, for structures with large damping ratios ξ_S, the structural displacements are similar regardless of the mass ratio, and therefore increasing the mass ratio is unlikely to reduce the structure's displacements.

6. Comparison of optimization methods

To get further insight into the effectiveness of the optimization process, this section compares the results from the PSO algorithm (Section 4) and from the optimization method proposed by Ricciardelli and Vickery [2]. This allows for quantitative comparisons between the optimum displacements and optimum FTMD parameters calculated by the optimization process, and a well-established method used in practical design. However, it should be mentioned that this comparison has some limitations due to the different optimization procedure adopted by Ricciardelli and Vickery and by this study. Indeed, Ricciardelli and Vickery proposed closed-form expressions to minimize the steady state response of a SDOF structure with FTMDs subjected to harmonic force. Ricciardelli and Vickery considered two cases: i) a system at resonance, and ii) a system subjected to an excitation with a varying frequency and constant amplitude. Ricciardelli and Vickery's method neglects the frequency content of the excitations, and therefore there is no difference between optimum parameters for different ground motions. In contrast, in the proposed PSO method, optimum parameters are calculated based on the excitation's frequency content, aiming to minimize the average response of the system.

A series of systems similar to that studied by Ricciardelli and Vickery are considered for comparison, with $T_s = 0.5$s and mass ratios $0.005 < \mu < 0.1$. Fig. 12 compares $x_{s,ave}$ of the above systems with FTMDs parameters f and R_f calculated using Ricciardelli and Vickery's method and with FTMDs parameters f and R_f optimized with the PSO algorithm. The average displacement of the uncontrolled system is 111.7 mm. The results in Fig. 12 show that both methods effectively reduce $x_{s,ave}$ and that the reduction in $x_{s,ave}$ increases with the mass ratio μ. However, compared to Ricciardelli and Vickery's optimization method, the PSO algorithm reduces the SDOF displacements $x_{s,ave}$ by an additional 21% on average. Such difference in results was somehow expected since Ricciardelli and Vickery's closed-form expressions are for optimizing FTMDs parameters of systems subjected to harmonic excitations, whereas the case studies examined in this article were subjected to ground motion excitations.

Fig. 12 also shows that the values f calculated by Ricciardelli and Vickery's method are always larger than those obtained with the PSO algorithm. However, optimum values of R_f given by both methods are relatively close to each other, especially in the case of $\mu > 0.06$. Based on

Table 3
Optimum parameters of FTMDs and TMDs.

T_s (s)	FTMD		TMD	
	f	R_f	f	ξ_T
0.5	0.929	0.194	0.928	0.043
1.0	1.054	0.057	1.023	0.050
4.0	1.062	0.012	1.019	0.028

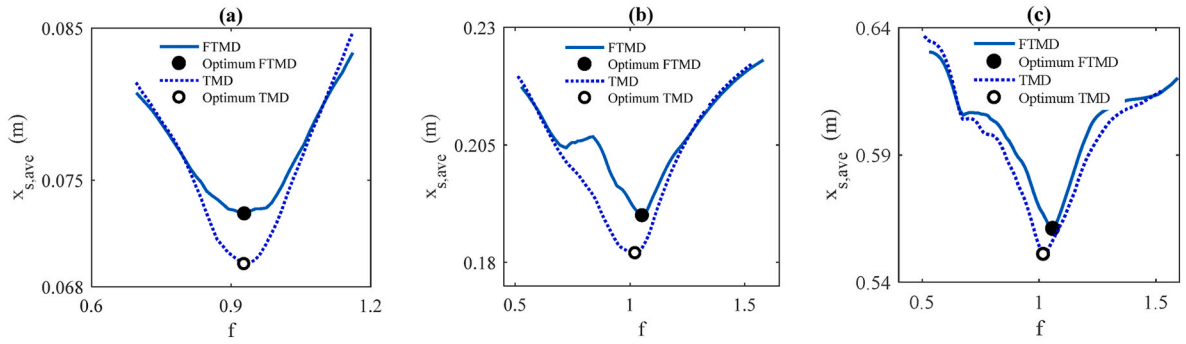

Fig. 7. Sensitivity of $x_{s,\mathrm{ave}}$ to variations in frequency ratio of systems with T_s = a) 0.5 s, b) 1.0 s, and c) 4.0 s.

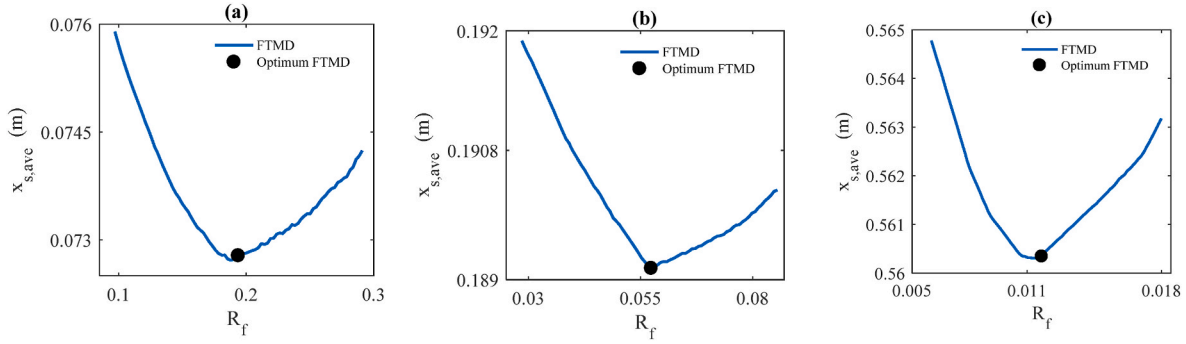

Fig. 8. Sensitivity of $x_{s,\mathrm{ave}}$ to variations in friction ratio of systems with FTMDs and T_s = **a) 0.5 s, b) 1.0 s, and c) 4.0 s.**

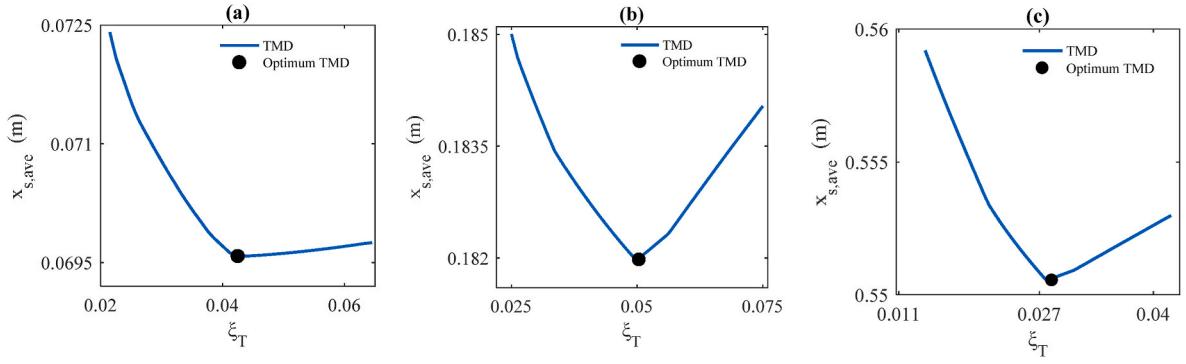

Fig. 9. Sensitivity of $x_{s,\mathrm{ave}}$ to variations in viscous damping ratio of systems with TMDs and T_s = **a) 0.5 s, b) 1.0 s, and c) 4.0 s.**

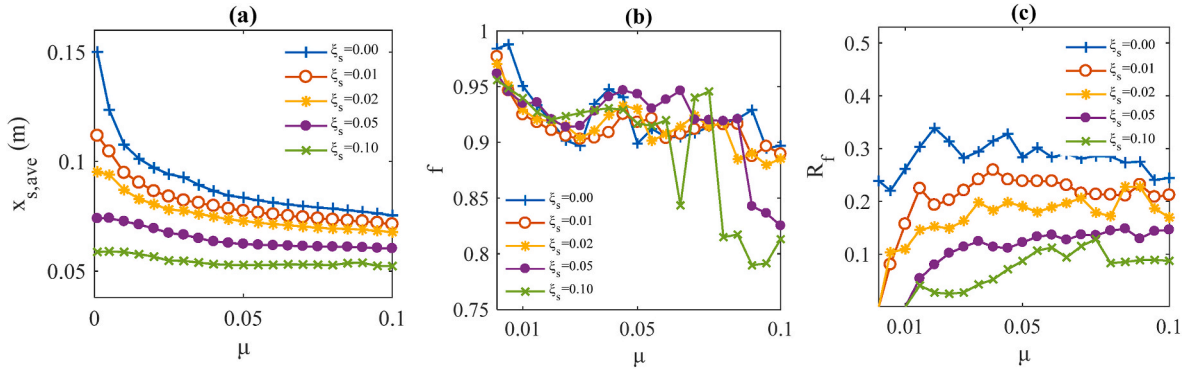

Fig. 10. (a) Optimum displacement $x_{s,\mathrm{ave}}$, (b) frequency ratio f, and (c) friction ratio R_f of systems with FTMDs for different damping ratio ξ_S of SDOF structure.

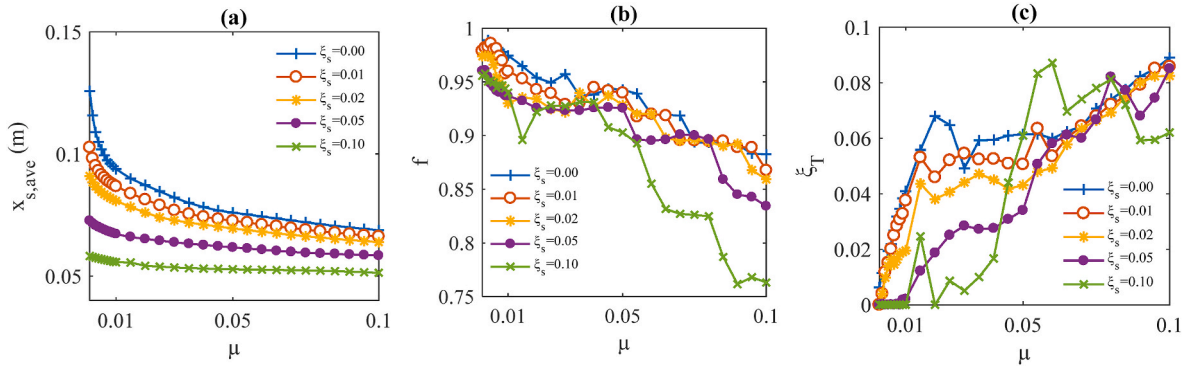

Fig. 11. (a) Optimum displacement $x_{s,ave}$, (b) frequency ratio f, and (c) damper damping ratio of systems with TMDs for different damping ratio ξ_S of SDOF structure.

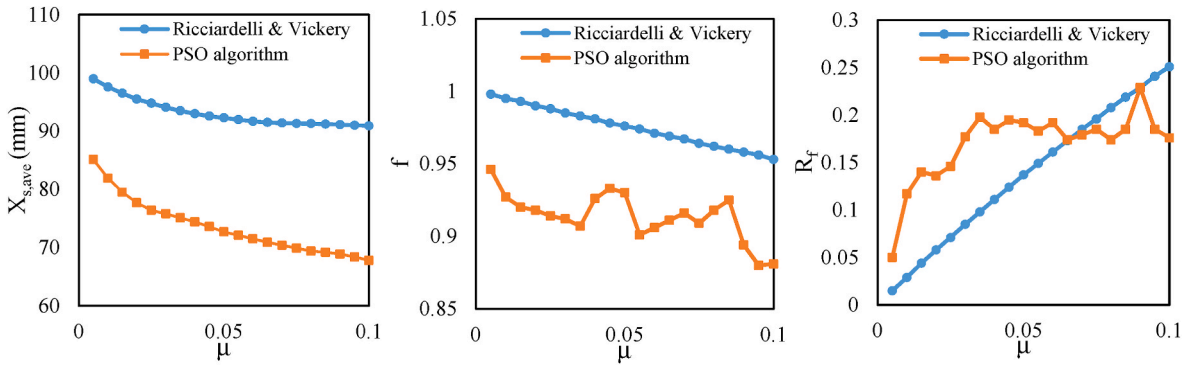

Fig. 12. Comparison of results from Ricciardelli and Vickery's and PSO optimization methods.

these results, it is possible to conclude that whilst Ricciardelli and Vickery method can be used to estimate optimum parameters, the PSO algorithm proposed here is more effective than their method at optimizing the SDOF displacements of the examined systems. Accordingly, PSO is a more effective option to optimize the response of structures with FTMDs. However, due to the limited number of systems, damper parameters and ground motion records considered in this study, further research should verify the validity of these conclusions to other case studies. It should be also noted that changes in the intensity of the ground motion records can change the results, especially in case of FTMDs with nonlinear behavior. Indeed, if a record set with a different hazard level is used in the optimization process, the optimum parameters would also change (especially the value R_f).

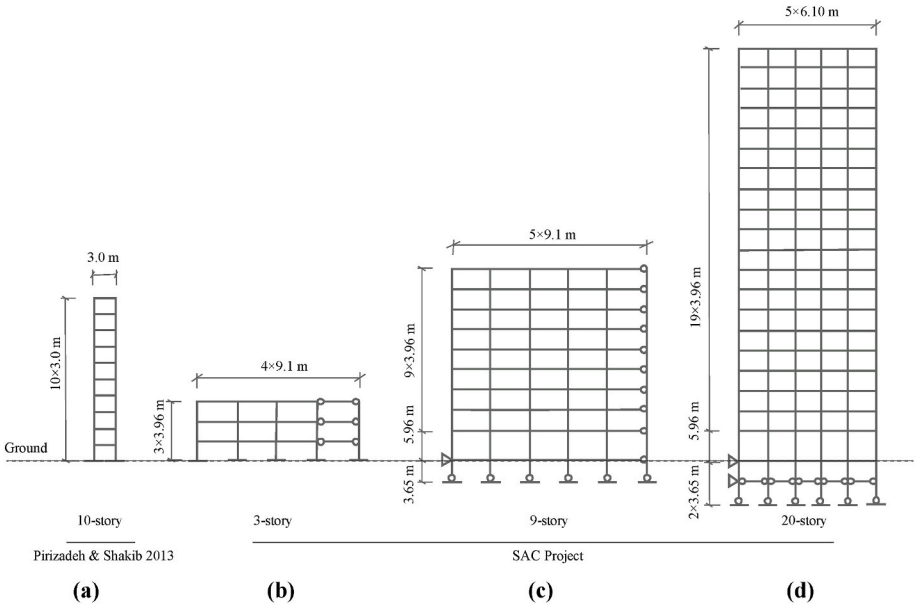

Fig. 13. Schematic elevation of moment-resisting frames.

7. Behavior of multi-story frame buildings with optimized FTMDs and TMDs

To investigate the effectiveness of FTMDs at controlling the displacements of multi-degree of freedom steel structures, a 10-story moment-resisting frame (fundamental period of 2.01 s) used by Pirizadeh and Shakib [45] was analyzed (Fig. 13a). Additionally, three regular moment-resisting frames from the SAC project [39] were also examined (Figs. 13b–d). The latter frames have 3, 9 and 20 stories, and fundamental periods of 1.01, 2.26 and 3.83 s, respectively. These frames have been used in previous research [46] to assess the effectiveness of vibration-control devices.

The above frames were modeled in OpenSees software [38] to perform nonlinear dynamic analysis. All frames were assumed as fixed at the base. The behavior of columns and beams was modeled using a Steel 02 material model. Likewise, the structural models were validated against the results presented in Refs. [39,45]. For each frame, it was assumed that FTMDs or TMDs were connected to the roof story level. For FTMDs, the mass was connected to the main structure by an elastic spring element and a rigid-plastic spring element working in parallel. In the case of TMDs, the mass was connected to the main structure by an elastic spring element and a viscous damper element working in parallel. To calculate the mass ratio μ, the mass of the main structure was considered as the mass of all stories above the ground level that are not restrained in the lateral direction. The viscous damping ratio of all frames was taken as 2%.

Table 4 presents the optimum response and damper parameters of FTMDs and TMDs connected to the frames. To find the optimum parameters of FTMDs and TMDs, the optimization procedure described in Section 4 was followed. Accordingly, the main objective was to minimize the maximum average displacement of the roof level of the frames when subjected to the full set of ground motion records (Table A.1 in Appendix A). The optimization variables were f and R_f for structures with FTMDs, and f and ξ_T for structures with TMDs. The optimization procedure was conducted for mass ratios ranging from 1% to 5%. The results in Table 4 are compared with the results in Table 1 and Table 3 for SDOF systems based on the fundamental period of the frames. Whilst this comparison has its own limitation (e.g. frames consider higher mode effects and nonlinear behaviour of materials), some general conclusions can be drawn. For example, increasing μ in both SDOF systems and frames resulted in increasing the percentage reduction of roof displacement. In the 3-story and 9-story frames, the percentage reduction of roof displacement was larger than their corresponding SDOF systems, whereas the opposite occurred in the 20-story frame. In the case of the 10-story frame, the roof displacement reduced by a similar percentage to the corresponding SDOF systems. This implies that the displacements predicted by SDOF systems match well the actual roof displacements of mid-rise height frames. In addition, changes of the percentage reduction of roof displacement for structures with TMDs and FTMDs show a similar trend. In most cases, however, the reduction is larger for structures with TMDs. The reduction also decreases for the 10-story and 20-story frames compared to the 3-story and 9-story frames. The results in Table 4 also provide some insight into the range of applicability of TMDs and FTMDs. For low-rise buildings, TMDs are often not an appealing solution due to their high cost. Moreover, the results in Table 4 indicate that, in high-rise buildings, TMDs and FTMDs reduce the seismic response only marginally. This is evident in the case of the 20-story frame, where the uncontrolled lateral displacement is small. As the behavior of this frame is practically linear, both TMDs and FTMDs are less effective at controlling lateral displacements.

A comparison of results in Table 3 and Table 4 also indicates that the optimum parameters of FTMDs and TMDs for SDOF systems and the studied frames are different. For example, the optimized frequency ratios f of FTMDs and TMDs for the 3-story frame were about 0.7, but the values f are always above one in its equivalent SDOF system. However, the optimum friction ratio R_f and viscous damping ratio ξ_T of FTMDs and TMDs in such a frame are close to their values in the equivalent SDOF system. In the case of the 20-story frame, the values f of FTMDs and TMDs are larger than their corresponding values in the equivalent SDOF system. Moreover, R_f and ξ_T of FTMDs and TMDs in this frame are zero, which means that damping in the added mass did not reduce the roof displacement. This is also observed in equivalent SDOF systems (Table 3), although in this case the ratios R_f and ξ_T are close to zero instead. Based on these results, it can be concluded that optimum friction ratios R_f and viscous damping ratios ξ_T obtained from SDOF systems represent good estimates for their corresponding ratios in real structural frames; however, this is not the case in optimum frequency ratios f. This also suggests that there are cases in which multi-story frame buildings cannot be simply represented by simple SDOF systems, especially if these are subject to real earthquakes. Finally, it should be noted that for the 3-story and 9-story frames (which experienced the best reduction in their response), the maximum displacements of the damper mass were 1.4 and 5.0 m respectively, which is acceptable for practical applications.

Table 4
Optimum FTMDs and TMDs fitted in moment-resisting frames.

Frame		μ	FTMD				TMD			
	Uncontrolled roof displacement (m)		f	R_f	Controlled roof displacement (m)	Percentage reduction (%)	f	ξ_T	Controlled roof displacement (m)	Percentage reduction (%)
3-story	0.191	1%	0.81	0.04	0.156	18.0	0.81	0.00	0.153	24.8
		2%	0.80	0.05	0.154	19.5	0.80	0.01	0.143	29.9
		3%	0.74	0.02	0.139	26.9	0.78	0.05	0.138	32.3
		4%	0.71	0.01	0.136	28.5	0.74	0.03	0.131	35.7
		5%	0.72	0.04	0.134	29.9	0.73	0.04	0.126	38.1
9-story	0.885	1%	1.01	0.00	0.778	12.1	0.95	0.03	0.774	12.5
		2%	1.04	0.07	0.751	15.1	0.95	0.06	0.702	20.7
		3%	0.97	0.13	0.732	17.3	0.95	0.08	0.648	26.8
		4%	0.73	0.11	0.700	20.9	0.96	0.08	0.614	30.6
		5%	1.12	0.02	0.628	29.1	0.94	0.11	0.586	33.8
10-story	0.402	1%	0.90	0.06	0.358	11.0	0.86	0.09	0.359	10.6
		2%	0.85	0.05	0.363	9.6	0.63	0.14	0.350	13.0
		3%	0.84	0.05	0.354	11.9	0.63	0.13	0.344	14.5
		4%	0.61	0.04	0.329	18.2	0.61	0.07	0.317	21.1
		5%	0.66	0.04	0.337	16.2	0.62	0.13	0.316	21.5
20-story	0.672	1%	0.92	0.00	0.664	1.1	1.27	0.00	0.663	1.3
		2%	1.11	0.00	0.655	2.5	1.36	0.00	0.654	2.6
		3%	1.12	0.00	0.647	3.7	1.26	0.00	0.646	3.8
		4%	1.25	0.00	0.638	5.0	1.26	0.00	0.638	5.0
		5%	1.24	0.00	0.631	6.1	1.25	0.00	0.631	6.1

It should be mentioned that whilst in this article the focus was on maximum average displacements, future research should investigate both the displacement and acceleration response in SDOF and MDOF systems with different properties and different types of FTDMs. This is particularly relevant for structures with short periods, where accelerations can be more relevant. Further research should also compare the robustness of TMDs and FTMDs by adopting a mechanical approach and frequency-based analyses.

8. Summary and conclusions

This article examined numerically the effectiveness of FTMDs at controlling the displacements of single degree of freedom systems subjected to real ground motion records. A PSO algorithm was adopted to find the optimized displacement of SDOF structures, as well as optimized parameters of FTMDs. For comparison, equivalent systems with TMDs were also optimized. Finally, a comparison was made between the above results and the results obtained for four multi-story moment-resisting frames. Based on the results of this study, the following conclusions are drawn:

1) The use of FTMDs is a feasible option to reduce the displacements of SDOF systems subjected to seismic records as those considered in this study.
2) Whilst optimized TMDs reduced the displacements more than FTMDs, the former reduces the SDOF displacements by an additional 6% on average. For both TMDs and FTMDs, the optimum frequency ratio as a function of the structure's period varies in a similar way. For the mass ratios considered in the PSO, the smaller scatter of friction ratio R_f in systems with FTMDs can be advantageous in practical design situations, where the main damper parameters may need to be tuned up to match the project needs.
3) Compared to the frequency ratio of TMDs, the frequency ratio of FTMDs is less sensitive to deviations from the optimum value. This makes FTMDs more attractive from an operational point of view. For design purposes, it is recommended to choose values of friction ratio R_f equal or higher than their optimized values.
4) FTMDs are effective at reducing the structure's displacement if the damping of the structure is low ($\xi_S < 0.02$). In this case, an increase in mass ratio leads to smaller structural displacements. However, in structures with high damping ($\xi_S = 0.1$), the use of FTMDs leads to similar structural displacements regardless of the mass ratio.
5) PSO is an attractive option to optimize the response of structures with FTMDs. For the structural systems examined in this study, the PSO algorithm reduces the SDOF displacements by an additional 21% on average when compared to Ricciardelli and Vickery's optimization method.
6) PSO can also be used to optimize the response of more complex structures with FTMDs. In addition, optimum friction ratios and viscous damping ratios obtained for SDOF systems can be used as good estimates for their corresponding ratios in real structural frames, but this is not acceptable for optimum frequency ratios. This also suggests that there are cases in which multi-story frame buildings cannot be represented by simple SDOF systems, especially if these are subjected to real earthquakes. This highlights the need for further studied in this area.

Declaration of competing interest

The authors declare that they have no known competing financial interests or personal relationships that could have appeared to influence the work reported in this paper.

Data availability

Data will be made available on request.

Appendix A

Table A.1
The selected SAC ground motion records for Los Angeles (probability of exceedance 10% in 50 years) with their dominant periods [31].

ID	Record Information	Mw	Period (sec)	PGA (g)
La01	Imperial Valley,1940,El Centro	6.9	0.52	0.46
La02	Imperial Valley,1940,El Centro	6.9	0.26	0.48
La03	Imperial Valley,1940,Array #05	6.5	0.16	0.39
La04	Imperial Valley,1940, Array #05	6.5	0.34	0.49
La05	Imperial Valley,1940, Array #06	6.5	0.06	0.3
La06	Imperial Valley,1940, Array #06	6.5	0.30	0.23
La07	Landers,1992,Barstow	7.3	0.72	0.42
La08	Landers,1992,Barstow	7.3	0.32	0.43
La09	Landers,1992,Yermo	7.3	0.68	0.52
La10	Landers,1992,Yermo	7.3	0.22	0.36
La11	Loma Prieta,1989,Gilroy	7.0	0.22	0.67
La12	Loma Prieta,1989,Gilroy	7.0	0.20	0.97
La13	Northridge,1994,Newhall	6.7	0.32	0.67
La14	Northridge,1994,Newhall	6.7	0.30	0.66
La15	Northridge,1994,Rinaldi RS	6.7	0.40	0.53
La16	Northridge,1994,Rinaldi RS	6.7	0.30	0.58
La17	Northridge,1994,Sylmar	6.7	0.32	0.57
La18	Northridge,1994,Sylmar	6.7	0.36	0.82
La19	North Palm Springs,1986	6.0	0.16	1.02
La20	North Palm Springs,1986	6.0	0.22	0.99

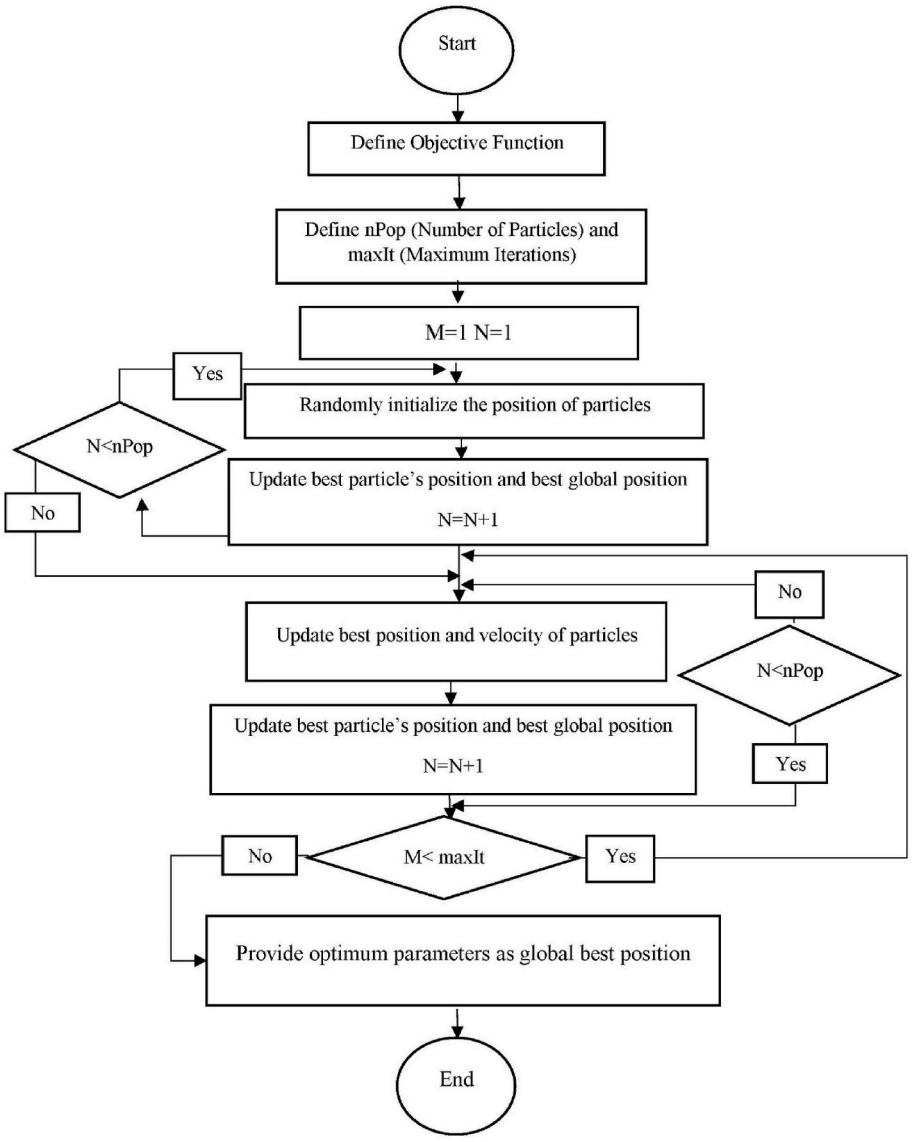

Fig. A1. Flowchart of PSO algorithm implementation

References

[1] Inaudi JA, Kelly JM. Mass damper using friction-dissipating devices. J Eng Mech 1995;121(1):142–9.
[2] Ricciardelli F, Vickery BJ. Tuned vibration absorbers with dry friction damping. Earthq Eng Struct Dynam 1999;28(7):707–23.
[3] Nasr A, Mrad C, Nasri R. Friction tuned mass damper optimization for structure under harmonic force excitation. Struct Eng Mech 2018;65(6):761–9.
[4] Lee JH, Berger E, Kim JH. Feasibility study of a tunable friction damper. J Sound Vib 2005;283(3–5):707–22.
[5] Lin CC, Lin GL, Wang JF. Protection of seismic structures using semi-active friction TMD. Earthq Eng Struct Dynam 2010;39(6):635–59.
[6] Lin GL, Lin CC, Lu LY, Ho YB. Experimental verification of seismic vibration control using a semi-active friction tuned mass damper. Earthq Eng Struct Dynam 2012;41 (4):813–30.
[7] Lupini A, Shim J, Epureanu BI. Experimental and computational study of a tuned damper with frictional contacts. AIAA J 2020;58(8):3607–13.
[8] Beskhyroun S, Wegner LD, Sparling BF. New methodology for the application of vibration-based damage detection techniques. Struct Control Health Monit 2012; 19(8):632–49.
[9] Xiang Y, Tan P, He H, Shang J, Zhang Y. Seismic optimization of variable friction pendulum tuned mass damper with hysteretic damping characteristic. Soil Dynam Earthq Eng 2022;160:107381.
[10] Matta E. Modeling and design of bidirectional pendulum tuned mass dampers using axial or tangential homogeneous friction damping. Mech Syst Signal Process 2019; 116:392–414.
[11] Matta E. A novel bidirectional pendulum tuned mass damper using variable homogeneous friction to achieve amplitude-independent control. Earthq Eng Struct Dynam 2019;48(6):653–77.
[12] Matta E. Bidirectional pendulum vibration absorbers with homogeneous variable tangential friction: modelling and design. J Struct Constr Eng 2018;12(11): 1074–82.
[13] Chung LL, Wu LY, Lien KH, Chen HH, Huang HH. Optimal design of friction pendulum tuned mass damper with varying friction coefficient, 20; 2013. p. 544–59.
[14] Gewei Z, Basu B. A study on friction-tuned mass damper: harmonic solution and statistical linearization. J Vib Control 2011;17(5):721–31.
[15] Pisal AY, Jangid RS. Dynamic response of structure with tuned mass friction damper. Int J Advert 2016;8(4):363–77.
[16] Dogan ME, Cigeroglu E. Vibration reduction by using two tuned mass dampers with dry friction damping. 1st Int Nonlinear Dynamic Conf (NODYCON) 2020;II: 59–67.
[17] Kim SY, Lee CH. Analysis and optimization of multiple tuned mass dampers with coulomb dry friction. Eng Struct 2020;209:110011.
[18] Jarrahi H, Asadi A, Khatibinia M, Etedali S. Optimal design of rotational friction dampers for improving seismic performance of inelastic structures. J Build Eng 2020;27:100960.

[19] Djerouni S, Abdeddaim M, Elias S, Rupakhety R. Optimum double mass tuned damper inerter for control of structure subjected to ground motions. J Build Eng 2021;44:103259.
[20] Salimi M, Kamgar R, Heidarzadeh H. An evaluation of the advantages of friction TMD over conventional TMD. Innov Infrastruct Solut 2021;6:95.
[21] Den Hartog JP. Mechanical vibrations. Courier Corporation; 1985.
[22] Miranda JC. Discussion of system intrinsic parameters of tuned mass dampers used for seismic response reduction. Struct Control Health Monit 2016;23(2):349–68.
[23] Sadek F, Mohraz B, Taylor AW, Chung RM. A method of estimating the parameters of tuned mass dampers for seismic applications. Earthq Eng Struct Dynam 1997;26(6):617–35.
[24] Warburton GB. Optimum absorber parameters for minimizing vibration response. Earthq Eng Struct Dynam 1981;9(3):251–62.
[25] Arfiadi Y, Hadi MN. Optimum placement and properties of tuned mass dampers using hybrid genetic algorithms. Iran J Mater Sci Eng 2011;1(1):167–87.
[26] Bekdaş G, Nigdeli SM, Yang XS. A novel bat algorithm based optimum tuning of mass dampers for improving the seismic safety of structures. Eng Struct 2018;159:89–98.
[27] Viana FA, Kotinda GI, Rade DA, Steffen Jr V. Tuning dynamic vibration absorbers by using ant colony optimization. Comput Struct 2008;86(13–14):1539–49.
[28] Yucel M, Bekdaş G, Nigdeli SM, Sevgen S. Estimation of optimum tuned mass damper parameters via machine learning. J Build Eng 2019;26:100847.
[29] Nigdeli SM, Bekdaş G. Optimum tuned mass damper design in frequency domain for structures. KSCE J Civ Eng 2017;21(3):912–22.
[30] Bakre SV, Jangid RS. Optimum multiple tuned mass dampers for base-excited damped main system. Int J Struct Stab 2004;4(4):527–42.
[31] Marano GC, Greco R, Chiaia B. A comparison between different optimization criteria for tuned mass dampers design. J Sound Vib 2010;329(23):4880–90.
[32] Leung AY, Zhang H. Particle swarm optimization of tuned mass dampers. Eng Struct 2009;31(3):715–28.
[33] Leung AY, Zhang H, Cheng CC, Lee YY. Particle swarm optimization of TMD by non-stationary base excitation during earthquake. Earthq Eng Struct Dynam 2008;37(9):1223–46.
[34] Hu X, Shi Y, Eberhart R. Recent advances in particle swarm. Proc. Congr Evol Comput 2004;1:90–7.
[35] De Domenico D, Qiao H, Wang Q, Zhu Z, Marano G. Optimal design and seismic performance of Multi-Tuned Mass Damper Inerter (MTMDI) applied to adjacent high-rise buildings. Struct Des Tall Special Build 2020;29(14):e1781.
[36] Marian L, Giaralis A. Optimal design of a novel tuned mass-damper inerter (TMDI) passive vibration control configuration for stochastically support-excited structural systems. Probabilist Eng Mech 2014;38:156–64.
[37] Wang Q, Qiao H, De Domenico D, Zhu Z, Tang Y. Seismic performance of optimal Multi-Tuned Liquid Column Damper-Inerter (MTLCDI) applied to adjacent high-rise buildings. Soil Dynam Earthq Eng 2021;143:106653.
[38] Mazzoni S, Mckenna F, Scott MH, Fenves GL. Open system for earthquake engineering simulation user command-language manual. Report NEES grid-TR 2004; 2006. p. 21.
[39] Gupta A, Krawinkler H. Seismic demands for performance evaluation of steel moment resisting frame structures (SAC Task 5.4.3). CA: John A. Blume Earthquake Engineering Center, Stanford University; 1999. Report No. 132.
[40] Decanini LD, Mollaioli F. An energy-based methodology for the assessment of seismic demand. Soil Dynam Earthq Eng 2001;21(2):113–37.
[41] Greco R, Marano GC. Optimum design of tuned mass dampers by displacement and energy perspectives. Soil Dynam Earthq Eng 2013;49:243–53.
[42] De Domenico D, Quaranta G, Ricciardi G, Lacarbonara W. Optimum design of tuned mass damper with pinched hysteresis under nonstationary stochastic seismic ground motion. Mech Syst Signal Process 2022;170:108745.
[43] Clerc M, Kennedy J. The particle swarm: explosion, stability, and convergence in a multi-dimensional complex space. IEEE Trans Evol Comput 2002;6:58–73.
[44] Soong TT, Spencer Jr BF. Supplemental energy dissipation: state-of-the-art and state-of-the-practice. Eng Struct 2002;24(3):243–59.
[45] Pirizadeh M, Shakib H. Probabilistic seismic performance evaluation of non-geometric vertically irregular steel buildings. J Constr Steel Res 2013;82:88–98.
[46] Matta E. Lifecycle cost optimization of tuned mass dampers for the seismic improvement of inelastic structures. Earthq Eng Struct Dynam 2018;47(3):714–37.